David B. Thiessen, et. al.. "Surface Tension Measurement."

Copyright 2000 CRC Press LLC. <http://www.engnetbase.com>.

Surface Tension Measurement

David B. Thiessen
California Institute of Technology

Kin F. Man
California Institute of Technology

The effect of surface tension is observed in many everyday situations. For example, a slowly leaking faucet drips because the force of surface tension allows the water to cling to it until a sufficient mass of water is accumulated to break free. Surface tension can cause a steel needle to "float" on the surface of water although its density is much higher than that of water. The surface of a liquid can be thought of as having a skin that is under tension. A liquid droplet is somewhat analogous to a balloon filled with air. The elastic skin of the balloon contains the air inside at a slightly higher pressure than the surrounding air. The surface of a liquid droplet likewise contains the liquid in the droplet at a pressure that is slightly higher than ambient. A clean liquid surface, however, is not elastic like a rubber skin. The tension in a piece of rubber increases as it is stretched and will eventually rupture. A clean liquid surface can be expanded indefinitely without changing the surface tension.

The mechanical model of the liquid surface is that of a skin under tension. Any given patch of the surface thus experiences an outward force tangential to the surface everywhere on the perimeter. The force per unit length of the perimeter acting perpendicular to the perimeter is defined as the *surface tension*, γ. Molecules in the interfacial region have a higher potential energy than molecules in the bulk phases because of an imbalance of intermolecular attractive forces. This results in an excess free energy per unit area associated with the surface that is numerically equivalent to the surface tension, as shown below. Consider a flat rectangular patch of fluid interface of width W and length L. In order to expand the length to $L + \Delta L$, an amount of work $\gamma W \Delta L$ must be done at the boundary. The product $W \Delta L$ is just the change in area ΔA of the surface. The work done to increase the area is thus $\Delta A \gamma$, which corresponds to the increase in surface free energy. Thus, the surface tension γ is seen to be equivalent to the surface free energy per unit area. Room-temperature organic liquids typically have surface tensions in the range of 20 mN m^{-1} to 40 mN m^{-1}, while pure water has a value of 72 mN m^{-1} at 25°C. The interface between two immiscible liquids, such as oil and water, also has a tension associated with it, which is generally referred to as the *interfacial tension.*

The surface energy concept is useful for understanding the shapes adopted by liquid surfaces. An isolated system in equilibrium is in a state of minimum free energy. Because the surface free energy contributes to the total free energy of a multiphase system, the surface free energy is minimized at
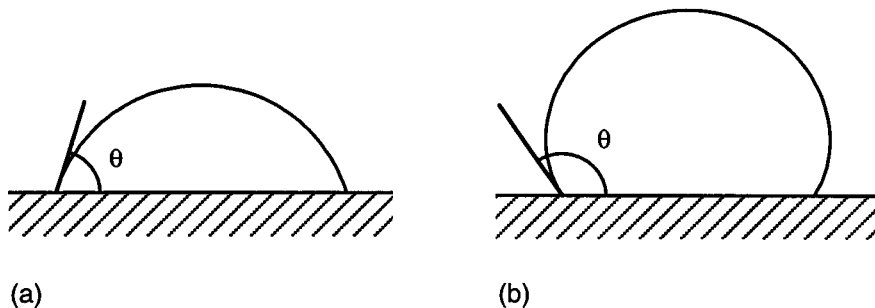
FIGURE 31.1 Illustration of contact angles and wetting. The liquid in (*a*) wets the solid better than that in (*b*).

equilibrium subject to certain constraints. Also, because the surface free energy is directly proportional to the surface area, surface area is also minimized. In the absence of gravity, a free-floating liquid droplet assumes a spherical shape because, for a given volume of liquid, the sphere has the least surface area. However, a droplet suspended from a needle tip on Earth does not form a perfect sphere because the minimum free energy configuration involves a trade-off between a reduction of the surface energy and a reduction of the gravitational potential. The droplet elongates to reduce its gravitational potential energy.

The surface energy concept is also useful for understanding the behavior of so-called surface active agents or *surfactants*. A two-component liquid mixture in thermodynamic equilibrium exhibits preferential adsorption of one component at the surface if the adsorption causes a decrease in the surface energy. The term surfactant is reserved for molecular species that strongly adsorb at the surface even when their concentration in the bulk liquid is very low. Surfactants are common in natural waters and are very important in many biological and industrial processes.

The interface between a solid and a fluid also has a surface free energy associated with it. Figure 31.1(*a*) shows a liquid droplet at rest on a solid surface surrounded by air. This system contains three different types of interfaces: solid–gas, solid–liquid, and liquid–gas, each with a characteristic surface free energy per unit area. The state of minimum free energy for the system then involves trade-offs in the surface area for the various interfaces. The region of contact between the gas, liquid, and solid is termed the *contact line*. The liquid–gas surface meets the solid surface with an angle θ measured through the liquid, which is known as the *contact angle*. The contact angle attains a value that minimizes the free energy of the system and is thus a characteristic of a particular solid–liquid–gas system. The system shown in Figure 31.1(*a*) has a smaller contact angle than that shown in Figure 31.1(*b*). The smaller the contact angle, the better the liquid is said to wet the solid surface. For θ = 0, the liquid is said to be perfectly wetting.

Measurement of surface tension is important in many fields of science and engineering, as well as in medicine. A number of standard methods exist for its measurement. In many systems of interest, the surface tension changes with time, perhaps, for example, because of adsorption of surfactants. Several standard methods can be used to measure dynamic surface tension if it changes slowly with time. Special techniques have been developed to measure dynamic surface tensions for systems that evolve very rapidly.

31.1   Mechanics of Fluid Surfaces

Some methods of measuring surface tension depend on the mechanics at the line of contact between a solid, liquid, and gas. When the system is in static mechanical equilibrium, the contact line is motionless, meaning that the net force on the line is zero. Forces acting on the contact line arise from the surface tensions of the converging solid–gas, solid–liquid, and liquid–gas interfaces, denoted by γ_{SG}, γ_{SL}, and γ_{LG}, respectively (Figure 31.2). The condition of zero net force along the direction tangent to the solid surface gives the following relationship between the surface tensions and contact angle θ:
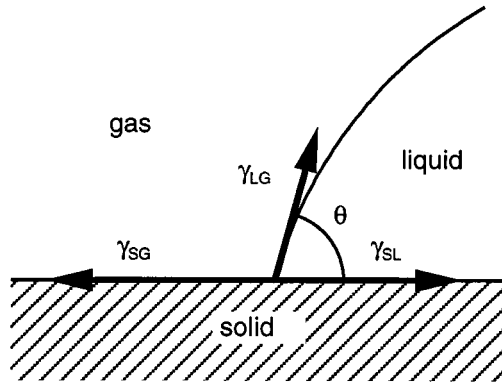
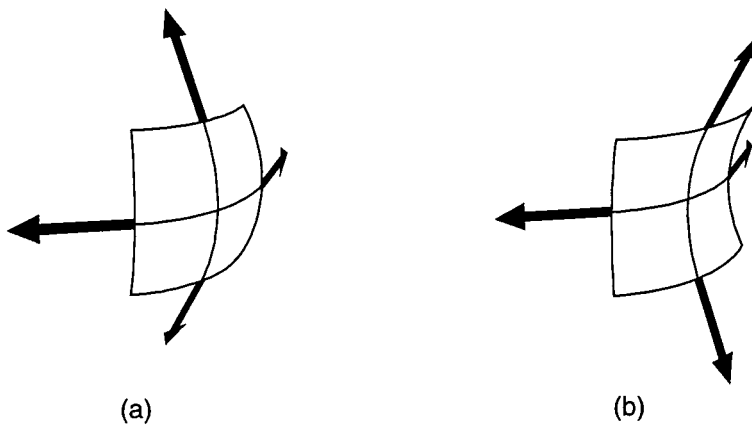**FIGURE 31.2**   Surface tension forces acting on the contact line.

(a)   **(b)**

FIGURE 31.3   Mechanics of curved surfaces that have principal radii of curvature of: (*a*) the same sign, and (*b*) the opposite sign.

$$\gamma_{SG} = \gamma_{SL} + \gamma_{LG} \cos\theta \qquad (31.1)$$

This is known as *Young's equation.* The contact angle is thus seen to be dependent on the surface tensions between the various phases present in the system, and is therefore an intrinsic property of the system.

As discussed in the introduction, the surface tension of a droplet causes an increase in pressure in the droplet. This can be understood by considering the forces acting on a curved section of surface as illustrated in Figure 31.3(*a*). Because of the curvature, the surface tension forces pull the surface toward the concave side of the surface. For mechanical equilibrium, the pressure must then be greater on the concave side of the surface. Figure 31.3(*b*) shows a saddle-shaped section of surface in which surface tension forces oppose each other, thus reducing or eliminating the required pressure difference across the surface. The mean curvature of a two-dimensional surface is specified in terms of the two principal radii of curvature, R_1 and R_2, which are measured in perpendicular directions. A detailed mechanical analysis of curved tensile surfaces shows that the pressure change across the surface is directly proportional to the surface tension and to the mean curvature of the surface:

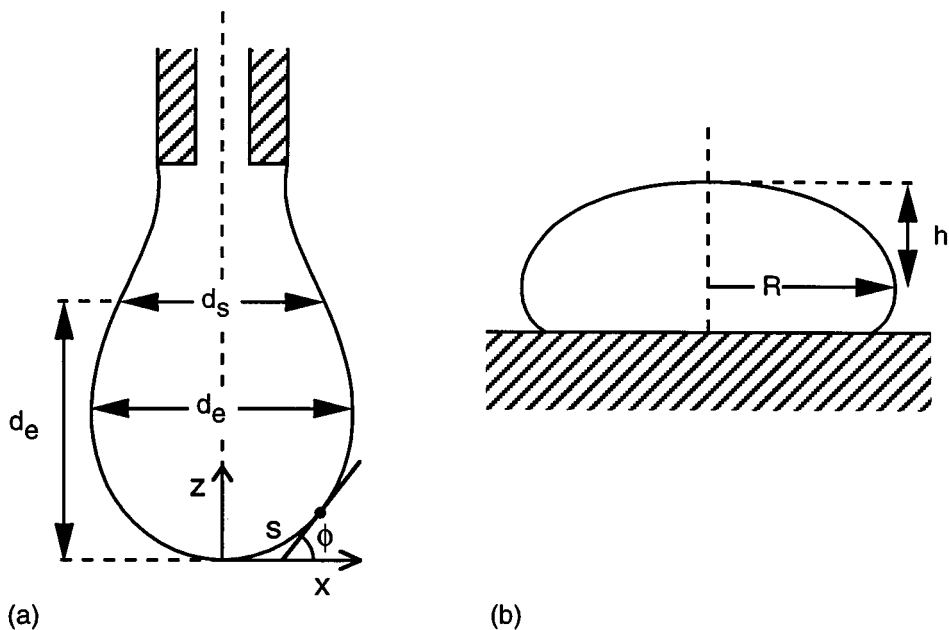$$P_A - P_B = \gamma\left(\frac{1}{R_1} + \frac{1}{R_2}\right) \qquad (31.2)$$

FIGURE 31.4 (*a*) A pendant drop showing the characteristic dimensions, d_e and d_s, and the coordinates used in the Young–Laplace equation. (*b*) A sessile drop showing the characteristic dimensions R and h.

where γ is the surface tension, and the quantity in brackets is twice the mean curvature. The sign of the radius of curvature is positive if its center of curvature lies in phase A and negative if it lies in phase B. Equation 31.2 is known as the *Young–Laplace equation*, and the pressure change across the interface is termed the *Laplace pressure*. Measurement of the Laplace pressure for a surface of known curvature then allows a determination of the surface tension.

Several methods of surface tension measurement are based on the measurement of the static shape of an axisymmetric drop or bubble or on the point of mechanical instability of such drops or bubbles. In a gravitational field a drop or bubble that is attached to a solid support assumes a nonspherical shape. Figure 31.4(*a*) shows the shape of a hanging droplet, also known as a pendant drop, and Figure 31.4(*b*) shows a so-called sessile drop. Axisymmetric air bubbles in water attain the same shapes as water drops in air, except that they are inverted. A bubble supported from below is thus called a hanging or pendant bubble, and a bubble supported from above is called a captive or sessile bubble. The reason for the deviation of the shape from that of a sphere can be understood from Equation 31.2. The hydrostatic pressure changes with depth more rapidly in a liquid than in a gas. The pressure difference across the surface of a pendant drop in air therefore increases from top to bottom, requiring an increase in the mean curvature of the surface according to Equation 31.2. The drop in Figure 31.4(*a*) has a neck at the top, which means that the two principal radii of curvature have opposite signs and cancel to some extent. At the bottom of the drop, the radii of curvature have the same sign, thus making the mean curvature larger. The Young–Laplace equation can be written as coupled first-order differential equations in terms of the coordinates of the interface for an axisymmetric surface in a gravitational field as:

$$\frac{dx}{ds} = \cos\phi$$

$$\frac{dz}{ds} = \sin\phi$$

(31.3)

$$\frac{d\phi}{ds} = \frac{2}{b} + \left(\frac{\Delta\rho g}{\gamma}\right)z - \frac{\sin\phi}{x}$$

$$x(0) = z(0) = \phi(0) = 0$$

where x and z are the horizontal and vertical coordinates, respectively, with the origin at the drop apex; s is the arc-length along the drop surface measured from the drop apex; and ϕ is the angle between the surface tangent and the horizontal (Figure 31.4(a)). The parameter b is the radius of curvature at the apex of the drop or bubble, $\Delta\rho$ is the density difference between the two fluid phases, and g is the acceleration of gravity. Numerical integration of Equation 31.3 allows one to compute the shape of an axisymmetric fluid interface. Comparison of computed shapes with experimentally measured shapes of drops or bubbles is a useful method of measuring surface tension. If all lengths in Equation 31.3 are made dimensionless by dividing them by b, the resulting equation contains only one parameter, $\beta = \Delta\rho g b^2/\gamma$, which is called the Bond number (or shape factor). The shape of an axisymmetric drop, bubble, or meniscus depends only on this one dimensionless parameter. The Bond number can also be written as $\beta = 2b^2/a^2$ where $a = \sqrt{2\gamma/\Delta\rho g}$ is known as the capillary constant and has units of length.

Several dynamic methods of measuring surface tension are based on capillary waves. Capillary waves result from oscillations of the liquid surface for which surface tension is the restoring force. The frequency of the surface oscillation is thus dependent on the surface tension and wavelength. Very low amplitude capillary waves with a broad range of frequencies are always present on liquid surfaces owing to thermal fluctuations. Larger amplitude capillary waves can be excited by purposely perturbing the surface.

31.2 Standard Methods and Instrumentation

A number of commonly used methods of measuring surface tension exist. The choice of a method depends on the system to be studied, the degree of accuracy required, and possibly on the ability to automate the measurements. In the discussion that follows, these methods are grouped according to the kind of instruments used in the measurements. Because the information presented for each method is necessarily brief, readers who are interested in constructing their own apparatus should consult the more detailed treatises in [1–4]. A list of commercially available instruments is given in Table 31.1, together with manufacturer names and approximate prices. Vendors can be contacted at the addresses given in Table 31.2.

TABLE 31.1 Commercially Available Instruments

Method	Instrument type	Manufacturer/Product name	Approximate price (range)
Capillary rise	Manual	Fisher	$79
Wilhelmy plate/du Noüy ring	Manual, mechanical balance	CSC, Fisher, Kahl	$2000–$4000
Wilhelmy plate/du Noüy ring	Manual, electrobalance	KSV, Lauda, NIMA	$4000–$11,000
Wilhelmy plate/du Noüy ring	Automatic, electrobalance	Cahn, Krüss, KSV, NIMA	$9000–$24,000
Maximum bubble pressure	Automatic	Krüss, Lauda, Sensa Dyne	$5000–$23,000
Pendant/sessile drop	Manual	Krüss, Rame-Hart	$7000–$10,000
Pendant/sessile drop	Automatic	ADSA, AST, FTA, Krüss, Rame-Hart, Temco	$10,000–$100,000
Drop weight/volume	Automatic	Krüss, Lauda	$16,000–$21,000
Spinning drop	Manual	Krüss	$20,100

Note: Price ranges reflect differences in degree of automation, the number of accessories included, or variation in price between manufacturers.

TABLE 31.2 Manufacturers and Suppliers of Instruments for Surface Tension Measurement

AST Products
9 Linnell Circle
Billerica, MA 01821-3902
Tel: (508) 663-7652

Applied Surface Thermodynamics Research
  Associates (ASTRA)
(distributor of ADSA instrumentation)
15 Brendan Rd.
Toronto, Ontario
Canada, M4G 2W9
Tel: (416) 978-3601

Brinkmann Instruments, Inc.
(distributor for Lauda tensiometers)
One Catiaque Road
P.O. Box 1019
Westbury, NY 11590-0207
Tel: (800) 645-3050

Cahn Instruments
5225 Verona Rd., Bldg. 1
Madison, WI 53711
Tel: (800) 244-6305

CSC Scientific Company, Inc.
8315 Lee Highway
Fairfax, VA 22031
Tel: (800) 458-2558

CTC Technologies, Inc.
(distributor for NIMA tensiometers)
7925-A North Oracle Road, Suite 364
Tucson, AZ 85704-6356
Tel: (800) 282-8325

First Ten Angstroms (FTA)
465 Dinwiddie Street
Portsmouth, VA 23704
Tel: (800) 949-4110

Fisher Scientific
711 Forbes Ave.
Pittsburgh, PA 15219-4785
Tel: (800) 766-7000

Kahl Scientific Instrument Corp.
P.O. Box 1166
El Cajon, CA 92022-1166
Tel: (619) 444-2158

Krüss U.S.A.
9305-B Monroe Road
Charlotte, NC 28270-1488
Tel: (704) 847-8933

KSV Instruments U.S.A.
P.O. Box 192
Monroe, CT 06468
Tel: (800) 280-6216

Rame-Hart, Inc.
8 Morris Ave.
Mountain Lakes, NJ 07046
Tel: (201) 335-0560

Sensa Dyne Instrument Div.
Chem-Dyne Research Corp.
P.O. Box 30430
Mesa, AZ 85275-0430
Tel: (602) 924-1744

Temco, Inc.
4616 North Mingo
Tulsa, OK 74117-5901
Tel: (918) 834-2337

Capillary Rise Method

If a glass capillary tube is brought into contact with a liquid surface, and if the liquid wets the glass with a contact angle of less than 90°, then the liquid is drawn up into the tube as shown in Figure 31.5(*a*). The surface tension is directly proportional to the height of rise, h, of the liquid in the tube relative to the flat liquid surface in the larger container. By applying Equation 31.2 to the meniscus in the capillary tube, the following relationship is obtained:

$$\Delta\rho gh = \frac{2\gamma}{b} \tag{31.4}$$

where b is the radius of curvature at the center of the meniscus and $\Delta\rho$ is the density difference between liquid and gas. For small capillary tubes, b is well approximated by the radius of the tube itself, assuming that the contact angle of the liquid on the tube is zero. For larger tubes or for increased accuracy, the
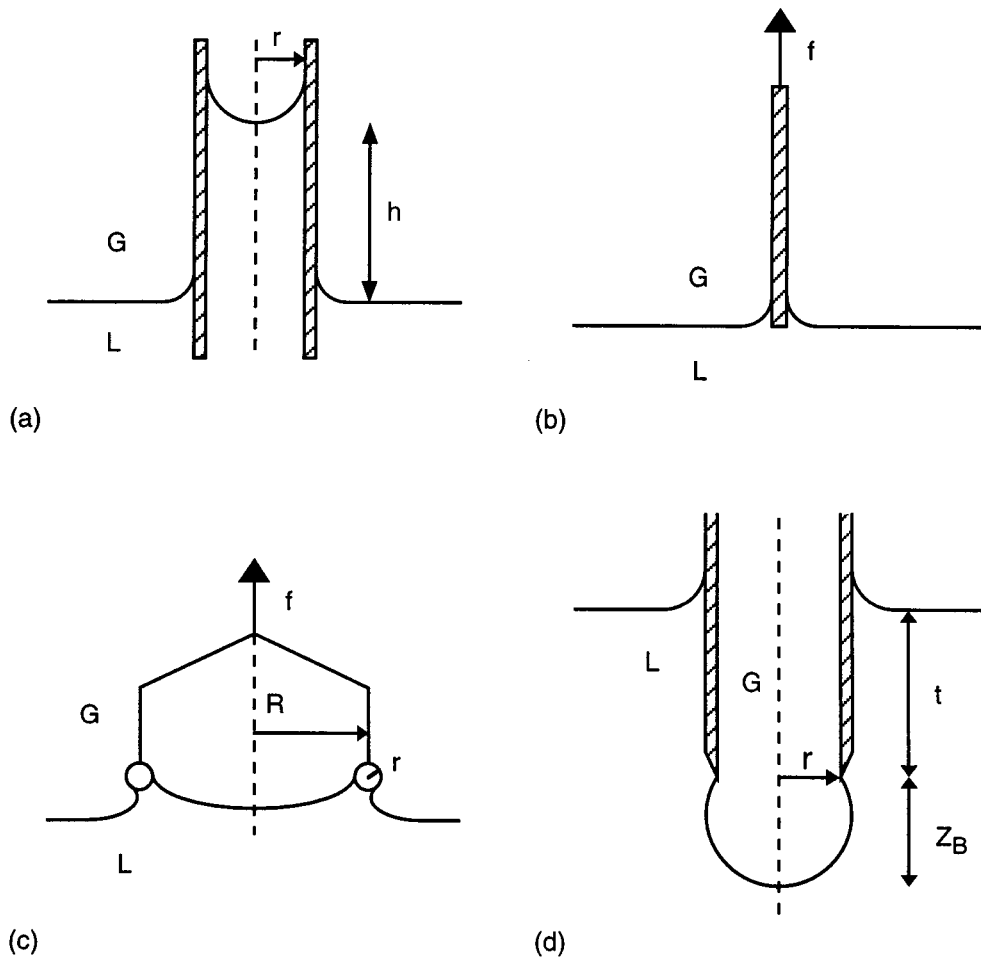
FIGURE 31.5 Geometries for: (*a*) capillary rise method, (*b*) Wilhelmy plate method, (*c*) du Noüy ring method, and (*d*) maximum bubble pressure method.

value of *b* must be corrected for gravitational deformation of the meniscus (p. 12 of [1]). Obtaining accurate results with the capillary rise method requires using a thoroughly clean glass capillary tube with a very uniform diameter of less than 1 mm. The container for the liquid should be at least 8 cm in diameter and the liquid must wet the capillary tube with a contact angle of zero. This method is primarily useful for pure liquids and is capable of high accuracy at relatively low cost.

Wilhelmy Plate and du Noüy Ring Methods

Measurement of the pull of a liquid surface directly on a solid object is the basis for two of the standard methods discussed here. In the Wilhelmy plate method, the solid object is a flat, thin plate that the test liquid should wet with a zero contact angle. The plate is suspended vertically from a delicate balance that is zeroed with the plate suspended in air. The test liquid is brought into contact with the bottom of the plate, causing the plate to be pulled down into the liquid by the surface tension force. The force applied to the plate from above is then increased to bring the bottom edge of the plate level with the flat surface of the liquid (Figure 31.5(*b*)). This avoids the necessity to make buoyancy corrections to the measurement. The surface tension is computed from the force measurement, *f*, using:

$$\gamma = \frac{f\cos\theta}{\left[2\left(l+t\right)\right]} \tag{31.5}$$

where l is the length of the plate and t is its thickness. The contact angle θ is often assumed to be zero for common liquids on clean glass or platinum plates, but one should be aware of the error caused by a non-zero contact angle. No other correction factors are necessary for this method and the fluid density does not need to be known.

The du Noüy ring method is known as a maximum pull method, of which there are several variations. The technique is to contact the liquid surface with a ring and then measure the force continuously as the surface is lowered until a maximum force, f_{max}, is recorded. The maximum force typically occurs just before the ring detaches from the surface. The surface tension is obtained from the formula:

$$\gamma = \left(\frac{f_{max}}{4\pi R}\right)\left[F\left(\frac{R^3}{V}, \frac{R}{r}\right)\right] \tag{31.6}$$

where R and r are the radii of the ring and wire, respectively, as indicated in Figure 31.5(*c*), V is the volume of liquid raised by the ring, and F is a correction factor (F is tabulated in Table 5, p. 132 of [4]). The du Noüy ring method requires knowledge of the liquid density, ρ_L, in order to determine V from $V = f_{max}/\rho_L$. This method requires the liquid to wet the ring with zero contact angle and is not suitable for solutions that attain surface equilibrium slowly.

A single instrument is normally capable of performing either Wilhelmy plate or du Noüy ring measurements. Some commercially available instruments can perform the complete measurement procedure automatically. Computer interfacing with a Wilhelmy plate instrument allows automatic data logging which can be used to follow changes in surface tension with time in surfactant solutions.

Maximum Bubble Pressure Method

The *maximum bubble pressure method* (MBPM) involves direct measurement of the pressure in a bubble to determine the surface tension. A tube is lowered to a depth t in the test liquid and gas is injected to form a bubble of height Z_B at the tip of the tube as shown in Figure 31.5(*d*). The increase in bubble pressure, P_b, over ambient pressure, P_a, arising from the interface is given by the sum of a hydrostatic pressure and Laplace pressure:

$$\delta p = P_b - P_a - \Delta\rho g t = \Delta\rho g Z_B + \frac{2\gamma}{b} \tag{31.7}$$

As a new bubble begins to form, Z_B increases while b, the radius of curvature at the bubble apex, decreases, resulting in an increase in pressure in the bubble. Ultimately, b increases as the bubble grows larger, thus reducing the pressure. The pressure in the bubble thus reaches a maximum when δp reaches a maximum, which in turn can be theoretically related to the surface tension. For $\delta p = \delta p_{max}$, Equation 31.7 can be rewritten in dimensionless form as follows:

$$\frac{r}{X} = \frac{r}{b} + \frac{r}{a}\frac{Z_B}{b}\left(\frac{\beta}{2}\right)^{1/2} \tag{31.8}$$

where r is the tube radius, X is a length defined as $X = 2\gamma/\delta p_{max}$, a is the capillary constant, and β is the Bond number. The dimensionless quantity r/X depends only on r/a, the relationship being determined by Equation 31.8 combined with numerical solutions of Equation 31.3. Tabulations of this relationship

are used to calculate the surface tension by an iterative procedure (p. 18 of [1]). The standard MBPM requires a knowledge of the fluid densities, tube radius, and depth of immersion of the tube.

A differential MBPM uses two tubes of different diameters immersed to the same depth. The difference in the maximum bubble pressure for the two tubes, ΔP, is measured, eliminating the need to know the immersion depth and making the method less sensitive to errors in the knowledge of the liquid density. For the differential MBPM, surface tension is computed from (see [5]):

$$\gamma = A\Delta P \left[1 + \left(\frac{0.69 r_2 \rho_L}{\Delta P} \right) \right]$$

(31.9)

where r_2 is the radius of the larger tube, ρ_L is the liquid density, and A is an apparatus-dependent constant that is determined by calibration with several standard liquids [6]. Automated MBPM units are commercially available (see Table 31.1). Sensa Dyne manufactures differential MBPM units that allow for on-line process measurements under conditions of varying temperature and pressure.

Pendant Drop and Sessile Drop Methods

The shape of an axisymmetric pendant or sessile drop (Figure 31.4) depends on only a single parameter, the Bond number, as discussed above. The Bond number is a measure of the relative importance of gravity to surface tension in determining the shape of the drop. For Bond numbers near zero, surface tension dominates and the drop is nearly spherical. For larger Bond numbers, the drop becomes significantly deformed by gravity. In principle, the method involves obtaining an image of the drop and comparing its shape and size to theoretical profiles obtained by integrating Equation 31.3 for various values of β and b. Once β and b have been determined from shape and size comparison, the surface tension is calculated from:

$$\gamma = \frac{\Delta \rho g b^2}{\beta}$$

(31.10)

In practice, the drop shape and size has traditionally been determined by the manual measurement of several characteristic dimensions (see Figure 31.4) of the drop from a photographic print. For pendant drops, the ratio d_s/d_e is correlated to a shape factor H from which surface tension is calculated (p. 27 of [3], [7]) according to:

$$\gamma = \frac{\Delta \rho g d_e^2}{H}$$

(31.11)

For sessile drops, various analytical formulae are available for computation of surface tension directly from the characteristic dimensions (p. 36 of [3]). Drop shape methods based on characteristic dimensions require very accurate measurement of the dimensions for good results. For more accurate results, methods that fit the entire shape of the edge of the drop to the Laplace equation are recommended.

In recent years, the entire procedure has been automated using digital imaging and computer image analysis [8, 9]. Typically, several hundred coordinates on the edge of the drop are located with subpixel resolution by computer analysis of the digital image. The size, shape, and horizontal and vertical offsets of the theoretical profile given by Equation 31.3 are varied by varying four parameters: b, β, and the pixel coordinates of the drop apex, x_0 and z_0. A best fit of the theoretical profile to the measured edge coordinates is obtained by minimizing an objective function. A digital image of a pendant drop can be analyzed for surface tension on a desktop computer in 1 or 2 s [10]. The speed of algorithms for pendant drop analysis on modern desktop computers has allowed this method to be used to track changes in surface tension for surfactant-covered surfaces by analyzing a sequence of images. The algorithms can simultaneously

track the surface area and volume of the drop or bubble. Both soluble and insoluble surfactants have been studied using the pendant drop, sessile drop, pendant bubble, and captive bubble configurations [11–13]. Table 31.1 lists several manufacturers that can provide software for automated analysis of surface tension from drops or bubbles in pendant or sessile configurations. The increased accuracy and simplicity of the automated pendant drop procedure makes it a very flexible method that has been applied to measure ultralow interfacial tensions, pressure, temperature and time dependence of interfacial tension, relaxation of adsorption layers, measurement of line tensions, and film-balance measurements [14].

Drop Weight or Volume Method

A pendant drop will become unstable and detach from its support if it grows too large. The weight of the detached portion is related to the surface tension of the fluid by:

$$\gamma = \left(\frac{mg}{r} \right) \left[F\left(\frac{r}{V^{1/3}} \right) \right] \tag{31.12}$$

where mg is the weight of the detached drop, r is the radius of the tip from which the drop hangs, and V is the volume of the detached drop. An empirical correction factor, F, is tabulated as a function of $r/V^{1/3}$ (p. 50 of [3]). For Equation 31.12 to apply, drops must be formed slowly. Measurements typically involve weighing the accumulated liquid from a large number of drops to determine the average weight per drop. The density of the fluid must be known in order to determine the drop volume and then obtain the factor F. Another method involves measuring the volumetric flow rate of liquid to the tip while counting the drops. The density of the fluid must be known in order to determine the drop weight. The latter method allows for automation of measurements [15].

Spinning Drop Method

The spinning drop method is a shape-measurement method similar to the pendant and sessile drop methods. However, the deformation of the drop in this case is caused by radial pressure gradients in a rapidly spinning tube. This method is normally used for measuring interfacial tensions between immiscible liquids. A horizontal glass tube with sealed ends is filled with the more dense liquid through a filling port. The tube is then spun about its axis while a drop of the lower density liquid is injected into the tube. The pressure in the outer liquid increases from the center of the tube toward the walls as a result of the spinning motion. The pressure gradient forces the drop to move to the center of the tube and causes it to elongate, while surface tension opposes elongation. Measurement of the maximum drop diameter, $2r_{max}$, and length, $2h_{max}$, together with the angular velocity of rotation, Ω, allows for calculation of the surface tension according to:

$$\gamma = \frac{1}{2} \left(\frac{r_{max}}{r_{max}^{\star}} \right)^3 \Delta\rho\Omega^2 \tag{31.13}$$

where $r_{max}^{\star}$ is correlated to the aspect ratio r_{max}/h_{max} [16]. The spinning drop method is particularly suited for measuring ultralow interfacial tensions (10^{-2} mN m^{-1} to 10^{-4} mN m^{-1}).

31.3   Specialized Methods

Dynamic Surface Tension

In an aqueous solution of soluble surfactant, the surface tension decreases following creation of new surface area because of adsorption of surfactant molecules. Surfactant adsorption kinetics can be studied

by measuring the change in surface tension with time. For a dilute solution, the rate of change of surface tension is often slow enough that automated versions of static methods such as the Wilhelmy plate or pendant drop [17] methods can be used to follow the changes in surface tension. In concentrated solutions in which large changes in surface tension can occur within a fraction of a second following surface creation, a dynamic method must be used. A liquid jet emerging from an elliptical orifice has stationary waves on its surface, the wavelengths of which are related to the surface tension. The oscillating jet method has been used to measure surface tension for surface ages as low as 0.6 ms [18]. A dynamic version of the maximum bubble pressure method has been used to measure dynamic surface tension at surface ages down to 0.1 ms [19].

Surface Viscoelasticity

A liquid surface covered by a monolayer of surfactant exhibits viscoelastic behavior. In addition to surface tension, the surface rheology is characterized in terms of dilatational and shear elasticities as well as dilatational and shear viscosities. The dilatational properties in particular are important in a variety of situations from foam stability to the functioning of the human lung. The surface dilatational modulus is proportional to the change in surface tension for a given change in surface area. This modulus depends on the rate of change of surface area for both soluble and insoluble surfactant monolayers, which indicates that relaxation processes are active. These relaxation processes give rise to the surface dilatational viscosity. For the case of soluble surfactants, one of the relaxation processes is the adsorption or desorption of molecules at the surface. The equilibrium dilatational elasticity of an insoluble monolayer can be measured by slowly expanding or compressing the monolayer in a Langmuir trough while monitoring the surface tension with a Wilhelmy plate apparatus [20]. Studies of surface rheology at high rates of surface expansion or compression are of interest for both soluble and insoluble surfactants.

Surface tension relaxation following sudden expansion or compression of the surface for a soluble surfactant has been studied by the automated pendant drop method [21]. A method known as oscillating bubble tensiometry has been applied to measure the kinetics of adsorption and desorption for soluble surfactants [22, 23]. Other methods for studying dynamic dilatational viscoelastic properties are reviewed in [24], including transverse and longitudinal capillary wave methods, a modified maximum bubble pressure method, and an oscillating bubble method.

Measurements at Extremes of Temperature and Pressure

Several of the standard methods described in this chapter can be adapted to make surface or interfacial tension measurements at extreme temperatures and/or pressures. The most common methods used to measure the surface tension of high-temperature molten metals, alloys, and semiconductors are the maximum bubble pressure method [25] and the pendant or sessile drop method [26–28]. Measurement of the interfacial tension between oil and a second immiscible phase at high pressure and elevated temperature is of interest for understanding aspects of enhanced oil recovery. The pendant drop method has been applied under pressures of 82 MPa at 449 K [29], while a capillary wave method has been applied at 136 MPa and 473 K [30]. A pendant drop apparatus capable of measurements to 10,000 psi (69 MPa) and 350°F (450 K) is commercially available from Temco Inc. (Table 31.2).

Interfacial Tension

Measurement of the interfacial tension between two immiscible liquids can present special difficulties. Measurement by the capillary rise, du Noüy ring, or Wilhelmy plate method is problematic in that the contact angle is often nonzero. The pendant drop [7] and drop weight [31] methods can both be applied, provided the densities of the two liquids are sufficiently different. The pendant drop method, in particular, is widely used for interfacial tension measurement. Interfacial tension can be measured by a modified maximum bubble pressure method in which one measures the maximum pressure in a liquid drop injected into a second immiscible liquid [32]. The modified maximum bubble pressure method [32] and

a liquid bridge method [33] have been used to measure interfacial tension between two liquids of equal density. Ultralow values of interfacial tension can be measured by the spinning drop [34], pendant drop [35], and capillary wave methods [34].

Defining Terms

Surface tension: A force per unit length that acts tangential to a liquid surface and perpendicular to any line that lies within the surface.

Surface energy: The excess free energy per unit area associated with a surface between two phases. For a liquid–fluid surface, the surface energy is numerically equivalent to the surface tension.

Acknowledgments

References

1. A. W. Adamson, *Physical Chemistry of Surfaces*, 5th ed., New York: John Wiley & Sons, 1990.
2. A. E. Alexander and J. B. Hayter, Determination of surface and interfacial tension, in A. Weissberger and B. W. Rossiter (eds.), *Physical Methods of Chemistry, Part V,* 4th ed., New York: John Wiley & Sons, 1971.
3. A. Couper, Surface tension and its measurement, in B. W. Rossiter and R. C. Baetzold (eds.), *Physical Methods of Chemistry, Vol. 9A,* 2nd ed., New York: John Wiley & Sons, 1993.
4. J. F. Padday, Surface tension. II. The measurement of surface tension, in E. Matijevic (ed.), *Surface and Colloid Science, Vol. 1,* New York: John Wiley & Sons, 1969.
5. S. Sugden, The determination of surface tension from the maximum pressure in bubbles. Part II, *J. Chem. Soc.*, 125, 27-31, 1924.
6. ASTM Standard D3825-90, Standard test method for dynamic surface tension by the fast-bubble technique, *1996 Annual Book of ASTM Standards, Vol. 05.02,* West Conshohocken, PA: ASTM, 1996, 575-579.
7. D. S. Ambwani and T. Fort, Jr., Pendant drop technique for measuring liquid boundary tensions, in R. J. Good and R. R. Stromberg (eds.), *Surface and Colloid Science, Vol. 11,* New York: Plenum Press, 1979.
8. Y. Rotenberg, L. Boruvka, and A. W. Neumann, Determination of surface tension and contact angle from the shapes of axisymmetric fluid interfaces, *J. Colloid Interface Sci.*, 93, 169-183, 1983.
9. P. Cheng, D. Li, L. Boruvka, Y. Rotenberg, and A. W. Neumann, Automation of axisymmetric drop shape analysis for measurements of interfacial tensions and contact angles, *Colloids Surf.,* 43, 151-167, 1990.
10. D. B. Thiessen, D. J. Chione, C. B. McCreary, and W. B. Krantz, Robust digital image analysis of pendant drop shapes, *J. Colloid Interface Sci.*, 177, 658-665, 1996.
11. S. Lin, K. McKeigue, and C. Maldarelli, Diffusion-controlled surfactant adsorption studied by pendant drop digitization, *AIChE J.,* 36, 1785-1795, 1990.
12. D. Y. Kwok, D. Vollhardt, R. Miller, D. Li, and A. W. Neumann, Axisymmetric drop shape analysis as a film balance, *Colloids Surf., A*, 88, 51-58, 1994.
13. W. M. Schoel, S. Schurch, and J. Goerke, The captive bubble method for the evaluation of pulmonary surfactant: surface tension, area, and volume calculations, *Biochim. Biophys. Acta*, 1200, 281-290, 1994.

14. S. Lahooti, O. I. Del Rio, P. Cheng, and A. W. Neumann, Axisymmetric drop shape analysis (ADSA), in A. W. Neumann and J. K. Spelt (eds.), *Applied Surface Thermodynamics*, New York: Marcel Dekker, 1996.

15. M. L. Alexander and M. J. Matteson, The automation of an interfacial tensiometer, *Colloids Surf.*, 27, 201-217, 1987.

16. J. C. Slattery and J. Chen, Alternative solution for spinning drop interfacial tensiometer, *J. Colloid Interface Sci.*, 64, 371-373, 1978.

17. D. Y. Kwok, M. A. Cabrerizo-Vilchez, Y. Gomez, S. S. Susnar, O. Del Rio, D. Vollhardt, R. Miller, and A. W. Neumann, Axisymmetric drop shape analysis as a method to study dynamic interfacial tensions, in V. Pillai and D. O. Shah (eds.), *Dynamic Properties of Interfaces and Association Structures*, Champaign, IL: AOCS Press, 1996.

18. W. D. E. Thomas and L. Potter, Solution/air interfaces. I. An oscillating jet relative method for determining dynamic surface tensions, *J. Colloid Interface Sci.*, 50, 397-412, 1975.

19. V. B. Fainerman and R. Miller, Dynamic surface tension measurements in the sub-millisecond range, *J. Colloid Interface Sci.*, 175, 118-121, 1995.

20. G. L. Gaines Jr., *Insoluble Monolayers at Liquid-Gas Interfaces*, New York: John Wiley & Sons, 1966, 44.

21. R. Miller, R. Sedev, K.-H. Schano, C. Ng, and A. W. Neumann, Relaxation of adsorption layers at solution/air interfaces using axisymmetric drop-shape analysis, *Colloids Surf.*, 69, 209-216, 1993.

22. D. O. Johnson and K. J. Stebe, Oscillating bubble tensiometry: a method for measuring the surfactant adsorptive-desorptive kinetics and the surface dilatational viscosity, *J. Colloid Interface Sci.*, 168, 21-31, 1994.

23. D. O. Johnson and K. J. Stebe, Experimental confirmation of the oscillating bubble technique with comparison to the pendant bubble method: the adsorption dynamics of 1-decanol, *J. Colloid Interface Sci.*, 182, 526-538, 1996.

24. D. A. Edwards, H. Brenner, and D. T. Wasan, *Interfacial Transport Processes and Rheology*, Boston: Butterworth-Heinemann, 1991.

25. C. Garcia-Cordovilla, E. Louis, and A. Pamies, The surface tension of liquid pure aluminium and aluminium-magnesium alloy, *J. Mater. Sci.*, 21, 2787-2792, 1986.

26. B. C. Allen, The surface tension of liquid transition metals at their melting points, *Trans. Metall. Soc. AIME*, 227, 1175-1183, 1963.

27. D. B. Thiessen and K. F. Man, A quasi-containerless pendant drop method for surface tension measurements on molten metals and alloys, *Int. J. Thermophys.*, 16, 245-255, 1995.

28. S. C. Hardy, The surface tension of liquid silicon, *J. Cryst. Growth*, 69, 456-460, 1984.

29. V. Schoettle and H. Y. Jennings, Jr., High-pressure high-temperature visual cell for interfacial tension measurement, *Rev. Sci. Instrum.*, 39, 386-388, 1968.

30. R. Simon and R. L. Schmidt, A system for determining fluid properties up to 136 MPa and 473K, *Fluid Phase Equilib.*, 10, 233-248, 1983.

31. K. Hool and B. Schuchardt, A new instrument for the measurement of liquid-liquid interfacial tension and the dynamics of interfacial tension reduction, *Meas. Sci. Technol.*, 3, 451-457, 1992.

32. A. Passerone, L. Liggieri, N. Rando, F. Ravera, and E. Ricci, A new experimental method for the measurement of the interfacial tension between immiscible fluids at zero Bond number, *J. Colloid Interface Sci.*, 146, 152-162, 1991.

33. G. Pétré and G. Wozniak, Measurement of the variation of interfacial tension with temperature between immiscible liquids of equal density, *Acta Astronaut.*, 13, 669-672, 1986.

34. D. Chatenay, D. Langevin, J. Meunier, D. Bourbon, P. Lalanne, and A. M. Bellocq, Measurement of low interfacial tension, comparison between a light scattering technique and the spinning drop technique, *J. Dispersion Sci. Technol.*, 3, 245-260, 1982.

35. D. Y. Kwok, P. Chiefalo, B. Khorshiddoust, S. Lahooti, M. A. Cabrerizo-Vilchez, O. Del Rio, and A. W. Neumann, Determination of ultralow interfacial tension by axisymmetric drop shape analysis, in R. Sharma (ed.), *Surfactant Adsorption and Surface Solubilization* (*ACS Symp. Ser. 615)*, Washington, D.C.: ACS, 1995, 374-386.